Structure Deformations and Existence of the α–β Transition in MXO₄ Quartz-like Materials

E. Philippot,[1] A. Goiffon, A. Ibanez, and M. Pintard

*Laboratoire de physicochimie des Matériaux solides, UM II, URA D0407-CNRS, cc 003, Place E. Bataillon,
F-34095 Montpellier cédex 5, France*

The paramount importance of M–X interactions in determining the existence or nonexistence of an α–β transition can be shown by a general survey of all known or predicted quartz-like materials, MXO_4. This distance, M–X, defined as the nonbonded radius sum, prescribes structure packing. If the M–O and X–O distances increase, intertetrahedron distortion will increase in relation to the decrease of the M–O–X angle, θ, and increase of the tilt angle, δ. From a structural point of view, a borderline value of $\delta \sim 22°$ or $\theta \sim 136°$ has been extrapolated for the existence of an α–β transition. © 1994 Academic Press, Inc.

INTRODUCTION

Research has been carried out over the past few years on MXO_4 quartz-like materials (M=B, Al, Ga, Fe, Mn and X=P, As). Their refined crystal structures (1) have been accurately defined, and investigations have begun into their crystal growth conditions (2–4) and piezoelectric properties (2, 4, 5–7). This has led to an investigation of the reverse growth process, in particular, controlled dissolution. This last process, as it concerns quartz, is essential for the manufacture of high-frequency resonator devices, as conventional mechanical lapping is not able to produce sufficiently thin samples (8–10).

During the course of this research, some similarities and some dramatic differences between the members of this series became apparent. For example, the continuous solid solution $Al_{(1-x)}Ga_xPO_4$ for $0 \leq x \leq 1$ (11) which always has the same cell volume, $V \sim 231$ Å³, confirms a very similar structural packing between both extreme compounds AlPO₄ and GaPO₄. From this analogy, it was possible to synthesize, by hydrothermal epitaxy, large as-grown crystals (5 to 8 cm long) of GaPO₄ from berlinite seeds (12). On the other hand, while berlinite exhibited an α–β transition as in quartz, this was absent in GaPO₄. These different behaviors have already been investigated

in some depth, in particular the management of the α–β transition and SiO₂ polymorphism (13). Quartz analogue studies have been less intensive (15–17). It is interesting to note that the α–β transition is always accompanied by an incommensurate intermediate phase which is close to the transition temperature (18, 19), and the question of whether this is order–disorder or displacive (13) is still being debated. Previous results are summarized in Table 1, together with those relating to GeO₂, which also has a quartz structure.

Although AlPO₄ and SiO₂ polymorphisms are closely related, those of the other compounds are more limited and varied. For example, the α–β transition is often missing. In this study, we will try to predict the existence of this transition in terms of structural constraints encountered in the quartz-like packing of all MXO_4 compounds.

I. Structural Modifications Related to the α–β Quartz Transition

The existence of this transition between low temperature α and high temperature β is only one example of the diversified polymorphism displayed by certain members of this series (Table 1). These transformations can be classified in two groups (13):

—Reconstructive transformations between very different structure packing phases (i.e., quartz and cristobalite structures);

—Distortive transformations for very slight atomic coordinate shifts (α–β quartz).

In this investigation of MXO_4 materials, we only take into account the second kind of transition and, more specifically, the connection existing between the structural distortion of the α-quartz packing related to the appearance of the transition to β-quartz.

One can easily understand how in quartz structure, the structure of the high temperature phase (β, space group $P6_422$) transforms into the low temperature phase (α, space group $P3_121$). Indeed, these two packings differ

TABLE 1

Polymorphism of All XO_2 and MXO_4 Compounds Derived from SiO_2

Compound	Structural type			Melting or decomposition	Ref.
	Quartz	Tridymite	Cristobalite		
BPO_4	α		β	>800°C	(17)
$BAsO_4$	α		β	>800°C	(17)
SiO_2	α $\xleftrightarrow{573°C}$ β	α $\xleftrightarrow{117°C}$ $β_1$ $\xleftrightarrow{163°C}$ $β_2$	α $\xleftrightarrow{220-270°C}$ β	1710°C	(14)
$AlPO_4$	α $\xleftrightarrow{586°C}$ β	$\xleftarrow{870°C}$ α $\xleftrightarrow{95°C}$ β $\xleftarrow{1400°C}$ $\xleftarrow{815°C}$ $\xrightarrow{1025°C}$	α $\xleftrightarrow{220°C}$ β	1600°C	(17, 20, 21)
$GaPO_4$		α $\xleftarrow{933°C}$ α	α $\overset{620}{\underset{560}{\rightleftharpoons}}$ β	1670°C	(17, 22, 23)
$MnPO_4$?		α $\xleftarrow{813°C}$ α			(16, 17)
GeO_2	α			1120°C	(24)
$FePO_4$	α $\xleftrightarrow{707°C}$ β			1240°C	(16, 17, 25)
$AlAsO_4$	(α $\xleftrightarrow{571°C}$ β)?			950°C	(26)
$GaAsO_4$	α			<1000°C	(15, 17)
$FeAsO4$	α?				(31)

Note. ? = Doubtful data.

from one another in a rotation, δ, of MO_4 and XO_4 tetrahedra around their twofold axis (Fig. 1a). This tilt or rotating angle δ has been defined by Grimm and Dorner for quartz structures (27), and has been extended to other quartz-like materials.

For β-quartz phase, less distorted tetrahedra exhibit angles, between O–O edges and z-axis, equal to 90 and ±45° and thus a zero value for the δ angle (Fig. 1b). For the less symmetrical α-phase, MO_4 and XO_4 tetrahedra are rotated around their twofold axes. In particular, the
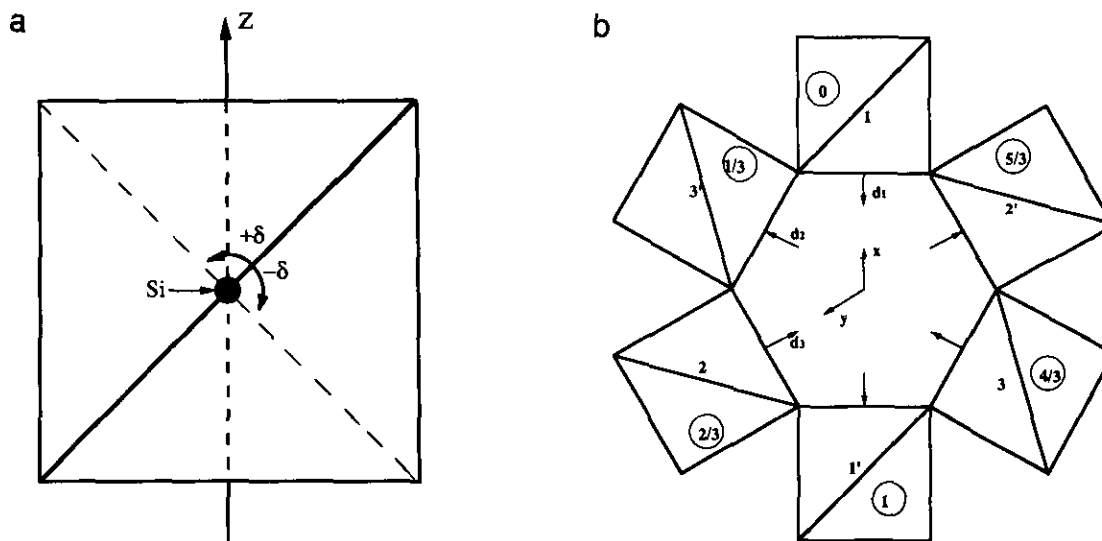

FIG. 1. (a) Projection of a SiO_4 tetrahedron, along a twofold axis of the β-quartz crystal structure, showing the two possibilities of rotation, ±δ, from β- to α-quartz structure. (b) Projection of β–quartz structure onto the x, y-plane. The values in circles show the relative height of M and X atoms above the x, y-plane. The tilt axes d_1–d_3 are indicated.

TABLE 2
Data of All Known Quartzlike Materials

	Tetrahedra	c/a	V (Å)	Bonds (Å)	[bonds] (Å)	δ (°)	[δ] (°)	$[\theta]_{theo.}$ (°)	$[\theta]_{exp.}$ (°)	d (Å) theo.	[M–X] exp.
BPO₄	BO₄ PO₄	2.22	171.8	*1.46* *1.52*	*1.48*		~20	~138		2.72	
BAsO₄	BO₄ AsO₄	2.26	186.2	*1.46* *1.70*	*1.58*		~15	~145		2.80	
SiO₂	SiO₄ 2×	1.10 2.20	113.0 226.0	1.608	1.608	16.3	16.3	144.8	143.7	3.06	3.057
AlPO₄	AlO₄ PO₄	2.21	231.5	1.736 1.521	1.628	16.2 18.9	17.6	142.8	142.4	3.08	3.085
GaPO₄	GaO₄ PO₄	2.25	229.2	1.815 1.525	1.670	20.8 25.7	23.3	135.4	134.6	3.09	3.085
GeO₂	GeO₄ 2×	1.13 2.26	121.7 243.4	1.739	1.739	25.7	25.7	131.7	130.1	3.16	3.153
FePO₄	FeO₄ PO₄	2.23	247.2	1.854 1.527	1.691	19.3 23.7	21.5	137.7	137.8	3.14	3.161
AlAsO₄	AlO₄ AsO₄	2.23	245.3	1.742 1.665	1.704	21.8 23.4	22.6	137.0	135.4	3.16	3.153
GaAsO₄	GaO₄ AsO₄	2.28	245.4	1.771 1.721	1.746	25.6 26.8	26.2	131.1	129.9	3.17	3.163
FeAsO₄	FeO₄ AsO₄	2.23	263.4	*1.85* *1.70*	*1.775*		~26.5	~130		3.22	

Note. Italics mean data from nonrefined crystal structures.

angle between the corresponding O–O edges and the z-axis is shifted from its ±45° value, and this shift is characterized by the tilt angle value, δ. As can be seen in Table 2 we have first calculated a mean value of this δ angle for each kind of tetrahedron, MO_4 and XO_4 (or YO_4 for SiO_2 and GeO_2), and then a final mean value of [δ] angle for both kinds of tetrahedra. Although the tetrahedra are not regular, we disregard the other small distortions in this section since they are insignificant compared to the total structural distortion. In these conditions, all known [δ] values are in the range 16.3° for SiO_2 to 26.2° for $GaAsO_4$.

On the other hand, the very close relationship between two possibilities of the rotating direction of δ and the kind of "Dauphiné" twin (or electrical twin), Fig. 1a, should be noted. This twin is closely related to the α–β transition and disappears for the β high temperature phase when δ = 0°. In some cases, the δ value has been measured as a function of temperature (SiO_2, $AlPO_4$, $GaPO_4$, and $AlAsO_4$ for $T \leq 800°C$ (27, 32–34)). First, this δ value decreases slowly until 500°C; then, it either continues in a similar manner to the final temperature, 800°C, for $GaPO_4$ and $AlAsO_4$, or quickly decreases to 0° for the SiO_2 and $AlPO_4$ transition.

After this brief review of the α–β transition, we shall

try to relate it to the crystal structure distortions of quartz and quartz-like materials.

II. Distortion of MXO₄ Structure Packing

First, we shall compare the structure packing of compounds $AlPO_4$ and $GaPO_4$, which are the most investigated, and then extend the results to all the other quartz-like materials.

II.1. Comparison of AlPO₄ and GaPO₄ α-quartz crystal structures. Although GaO_4 tetrahedra are larger than those of AlO_4 (Al–O = 1.736 Å and Ga–O = 1.815 Å), α-quartz structures of $AlPO_4$ and $GaPO_4$ show the same cell volume ($V = 231$ Å³), which remains constant for the whole continuous solid solution $Al_{(1-x)}Ga_xPO_4$. This preservation of the cell volume is explained by a weak and opposite evolution of a and c parameters which follow Vegard's law, the c/a ratio exhibiting a linear behavior in x (11). Then, as cell volumes and atomic coordinates of M and X atoms are very similar, the crystal structure of $GaPO_4$ must be more distorted than that of $AlPO_4$ (Fig. 2). This deformation leads to a lowering of the [M–O–X] angle, θ, from 142.4° for Al–O–P to 134.6° for Ga–O–P. In the same way, we observe an increase of the δ angle
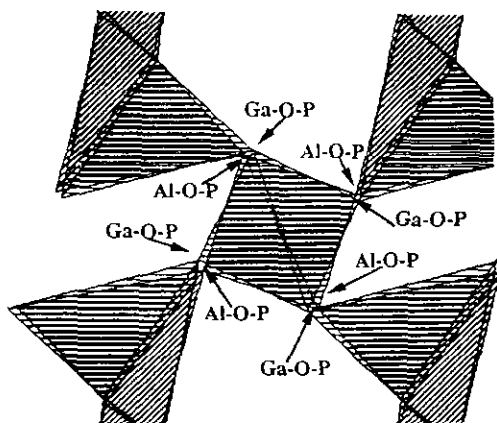
FIG. 2. Overlap of GaPO₄ and AlPO₄ crystal structures along the x-axis, showing the decreasing value of the bridging angles, Ga–O–P, compared to the Al–O–P angles.

value of MO_4 tetrahedra from 16.2° for AlO_4 to 20.8° for GaO_4 and, in a parallel direction, that of PO_4 tetrahedra from 18.9 to 25.7°. Then, the lengthening of the M–O bonds induces some structural alterations of MO_4 packing, as shown in Fig. 3, in which one tetrahedron rotation is compensated by those of the four neighboring tetrahedra in the opposite direction. This distortion is even more emphasized as it is cumulative, i.e., there is no alternation of MO_4 and XO_4 tetrahedra along the a-axis direction (Fig. 4). The increase of the δ value explains the more important distortion of the GaPO₄ crystal structure. This structural difference can explain the strong strains encountered in the epitaxial process of berlinite seeds by gallium phosphate, as shown later.

The geometrical equation relating θ and δ angles has been established by Grimm and Dorner (27) for quartz. Assuming regular SiO₄ tetrahedra, they have found the relation

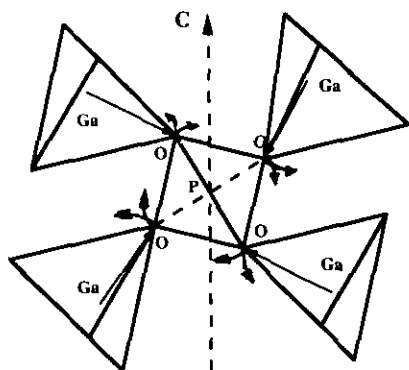$$\cos \theta = \tfrac{3}{4} - [\cos \delta + \tfrac{1}{2}\sqrt{3}]^2. \qquad [1]$$

FIG. 3. Influence of the lengthening of M–O bonds, from M=Al to Ga, giving an opposite rotation of AlO₄ and GaO₄ tetrahedra.
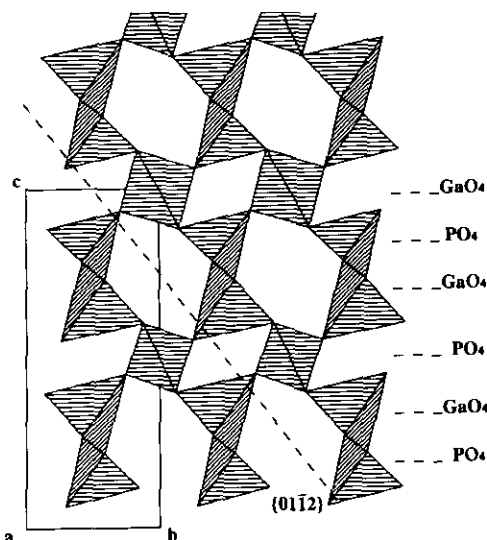

FIG. 4. Projection of GaPO₄ crystal structure along the a-axis, showing the preferential cracks, parallel to the (01̄12) planes.

As seen in Table 2, this equation is also verified for more distorted structures such as AlPO₄ and GaPO₄. Indeed, the θ_{theo} value, calculated from Eq. [1], concurs with the experimental one, θ_{exp}.

Nevertheless, one question is not solved: why does a more bulky GaO₄ tetrahedron lead, for GaPO₄, to the same cell volume as that of AlPO₄? One answer can be given from the works of Bragg (35), Bartell (36), and Glidewell (37), which have been expanded by O'Keeffe and Hyde (38, 39) to the crystal chemistry study of some silicates and other tetrahedral compounds. It must be specified that this approach is only valid for crystal structures based on chains of corner-sharing tetrahedra (and no edge-sharing tetrahedra), and for only the first three rows of the periodic classification as it is found in quartz-like crystals. The basic concept is derived from a compilation of numerous crystal structures in which the non-bonded distance Si–Si is always close to 3.06 Å whatever the value of the bridge Si–X–Si angle (with X = O, C, N) (Fig. 5). From this point of view, the predominant homopolar interactions in this packing are not due to the anion–anion interactions but to the cation–cation ones, and these cations are considered to be in contact. These results have been confirmed through crystal structure refinements of samples under pressure, in which a much more important shortening of anion–anion distances than the cation–cation one are observed. A typical radius, "nonbonded" or "one-angle radius" (38, 39), of 3.06/2 = 1.53 Å can be defined. Compilation has been expanded to other elements in tetrahedral coordination, and the corresponding values are listed in Table 3.

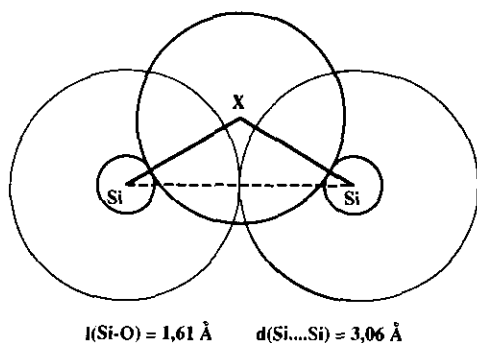From this table, it can be observed that gallium and

l(Si-O) = 1,61 Å   d(Si....Si) = 3,06 Å

FIG. 5. Cation–cation interactions from O'Keeffe (39). Heavier circles represent ionic radii from Shannon (40) and lighter circles represent "one angle" or "nonbonded" radii. The heavy full lines represent the X–O bonds, with X==(O, C, N), and the heavy dotted line the contact distance, d(Si ··· Si).

aluminum show similar nonbonded radii (1.63 and 1.62 Å, respectively). The phosphorus value being 1.46 Å, we find similar distances between nonbonded atoms P–Ga and P–Al (3.09 and 3.08 Å, respectively), which explain the constant cell volume for all the $Al_{(1-x)}Ga_xPO_4$ compositions. Then, as Ga–O bond distances are longer than the Al–O ones, we observe a decreasing value of the θ angle and, on the contrary, an increase of the δ angle, which demonstrates a greater distortion of $GaPO_4$ crystal structure.

In brief, M and X "cations" determine the cell volume of these materials through their repulsions (nonbonded radii), whereas the anion–cation interactions only influence intertetrahedral distortions (bridging angle θ and rotating angle δ) through the bond lengths (M–O and X–O), i.e., through the atomic size (ionic or covalent radii). We tested these ideas by extension to all the other quartz-like materials.

II.2. *Compared crystal structure data of all quartzlike materials, MXO_4.* Crystal structure data of all known quartz-like materials are summarized in Table 2 (1, 29, 30).

TABLE 3
Nonbonded Radii of Tetrahedral
Elements from Ref. (38)

Atom	Nonbonded radii (Å)
B	1.26
O	1.12
Al	1.62
Si	1.53
P	1.46
Ga	1.63
As	1.54
Fe^{III}	1.68

[In italics: unrefined crystal structures of BPO_4, $BAsO_4$, $MnPO_4$, and the hypothetical $FeAsO_4$. The bond lengths have been computed from Shannon's radii (40)]

In Table 2, c/a is the cell parameter ratio (must be multiplied by 2 for quartz and GeO_2). From a general point of view, Smith (41) has demonstrated that the c/a ratio must be equal to 1.098 [$c/a = \frac{3}{2} (\sqrt{3} - 1)$] for a "regular" β–quartz structure (2.196 for MXO_4). The more the c/a value increases, the more the structure is distorted compared to that of the regular β–quartz. V is the cell volume in $Å^3$ (must be multiplied by 2 for quartz and GeO_2). "Bonds" are the mean values of M–O and X–O bonds in Å and [bonds], the mean values of [(M–O) + (X–O)]/2 bond lengths in Å. δ is the "tilt angle" or rotating angle, in degrees, between β–quartz and α–quartz structures for each kind of tetrahedron, and [δ], its mean value for a crystal structure. [θ] is the theoretical (calculated from Eq. [1]) and experimental mean values of the bridging angle M–O–X, and d is the theoretical cation–cation distance calculated from nonbonded atomic radii (Table 3) and the corresponding experimental distance.

All known crystal structures exhibit constant cell volumes classified in two principal groups (~230 and ~245 $Å^3$), in agreement with previous works by O'Keeffe *et al.*, who estimate the nonbonded atom prevalence for the structure packing. Indeed, it can be observed for both series that the sum of the nonbonded radii M ··· X is constant, and that the theoretical and experimental values are in very good agreement.

On the other hand, as previously mentioned, the oxygen atoms are directly related to the structure packing distortion through their bond lengths M–O and X–O. In both the series with similar cell volume and similar nonbonded radius sum, the c/a ratio increases and the M–O–X angle, θ, decreases in terms of the bond mean value. [(M–O) + (X–O)]/2, deviating increasingly from $c/a = 2.196$ and $\theta_{theo} = 153°$, the "ideal" values for high temperature β–quartz (28, 42). This distortion can be related to an increase in "tilt angle," δ, which is representative of the MO_4 and XO_4 tetrahedron rotation, around their twofold axes, from the ideal β–quartz structure (Fig. 1a). For $AlPO_4$ and $GaPO_4$, from a geometrical point of view, this rotation is greater for smaller tetrahedra. For $AlPO_4$ and $AlAsO_4$ with similar AlO_4 tetrahedra, the δ value is greater for $AlAsO_4$, which is more distorted. The same can be said for $GaPO_4$ and $FePO_4$, which present similar PO_4 tetrahedra.

As can be verified in Table 2, the theoretical value of θ, calculated from Eq. [1], is always close to the experimental one derived from crystal structure refinements (Fig. 6). The validity of this relationship has been confirmed from structural studies of α–quartz and GeO_2 under pressure (24). Even for more distorted packing than those found in quartz structure, the θ_{theo} and θ_{exp} values remain
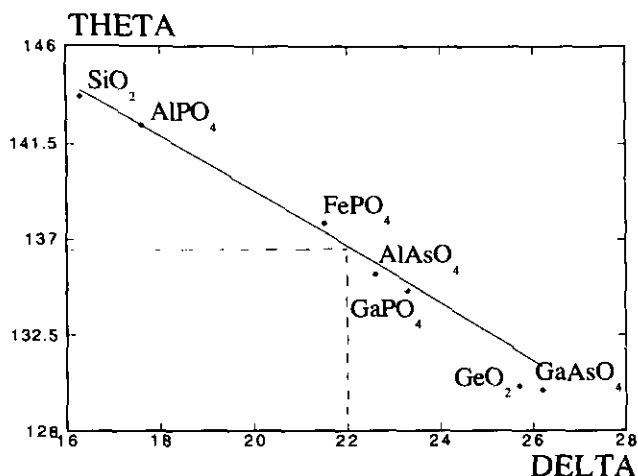
FIG. 6. Evolution of the bridging angle M–O–X, θ, in terms of the mean value of the distortion angle, δ, of MO₄ and XO₄ tetrahedra. The theoretical evolution from Eq. [1] is given in full line. The α ↔ β–quartz transition disappears for a θ value ~136° and a δ value ~22°.

in good agreement for more distorted tetrahedra, as seen in all known MXO₄ structures. Then, the intratetrahedron distortion effect is negligible, even if the mean value, [δ], takes this partly into account.

Having compared all known quartz-like structures, we now try to relate structural distortion and α–β transition existence, and to predict the unknown behavior of some compounds.

III. Prediction of α–β Transition for Quartzlike Materials

Equation [1] is always true for all quartz-like materials, as shown in Fig. 6; the mean value of the tetrahedron tilt angle, δ, presents a linear variation in terms of the bridging angle M–O–X, θ, between two corner-sharing tetrahedra. Similarly, this δ angle exhibits a linear variation in terms of the mean bond length, [(M–O) + (X–O)]/2 for the phases having a constant cell volume (Fig. 7). From both Figs. 6 and 7, the α–β transition disappearance is close to [δ] ~ 22° (or θ ~ 136°). Lower δ values for SiO₂, AlPO₄, and FePO₄ promote its existence, whereas it disappears for higher values for GaPO₄, GeO₂, and GaAsO₄. The energy needed to increase the M–O–X angle to θ ~ 153° (M–O–X value for β–quartz structure), or to reduce tilt angle δ to 0°, increases with structural distortion. This result concurs with thermodynamic calculations from Krempl et al. (43) which predict very high theoretical temperatures of the α–β transition for AlAsO₄ (1140°C), GaPO₄ (1656°C), and GaAsO₄ (1503°C). Then, for these compounds, other transitions(α-quartz → cristobalite at T = 933°C) or chemical decompositions (950°C for AlAsO₄ and <1000°C for GaAsO₄ (15)) can be observed before the α–β quartz transition.

One study (26) has reported the transition for AlAsO₄. Considering its [δ] value, 22.6°, close to the borderline value, [δ ~ 22°], it is possible that the α–β transition could have been aided by the presence of impurities.

As already mentioned, Young (44) has shown the close relation between the rotating direction of δ and the kind of "Dauphiné" twin. As the transition disappears for the high values of tilt angle, it can be assumed that the simultaneous existence predicted for both kinds of twins must be lowered as the energy needed for the transfer between both configurations is increased. Though inconsistent with a previous work (45), our crystal growth experiments corroborate this hypothesis as, in contrast to the less distorted material AlPO₄, this kind of twin is much more unusual in as-grown GaPO₄ crystals. (On the other hand, cracks are more frequent in GaPO₄ than in AlPO₄ for structural distortion purposes.)

Finally, there are still some problems connected with the compounds for which the data are given in italics in Table 2. Their α-quartz phase has been isolated and their cell parameters given, but their crystal structure and their complete polymorphism are unknown. Their theoretical angles, [δ] and [θ], calculated from their nonbonded radii (Table 3), suppose the possible existence of an α–β transition. For BPO₄ and BAsO₄, with δ values less than 22°, this must be probable, but on the contrary, this δ value is much too high for the FeAsO₄ phase.

It is doubtful that the α-quartz phase of FeAsO₄ and MnPO₄ exists, even though each one has been observed on one occasion. For FeAsO₄, as for AlAsO₄, the problem

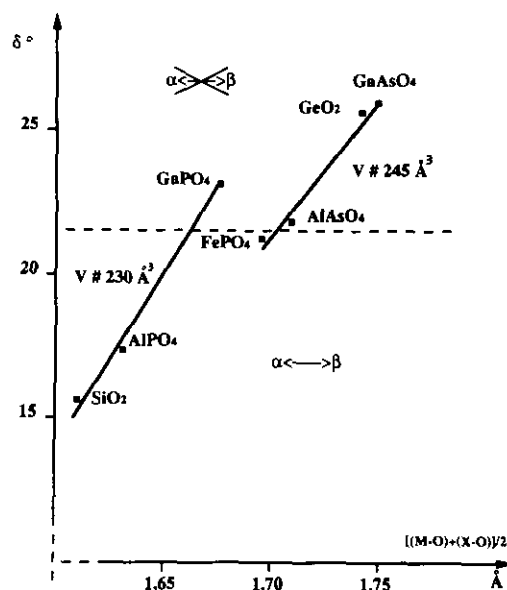FIG. 7. Evolution of the distortion angle, δ, in terms of the mean value of the bond [(M–O) + (X–O)]/2. The α ↔ β–quartz transition disappears for a δ value ~22°.

can be a purity one. On the other hand, for $MnPO_4$, we are not aware of fourfold coordination of Mn^{III} (40).

CONCLUSION

In their paper on the $\alpha-\beta$ quartz transition, Grimm and Dorner (27) conclude that the role of nonbonded Si–Si interactions is of prime importance in this process. The generalizations, considered in this study, confirm that the $M-X$ distance controls the existence or nonexistence of this transition for all quartz-like materials.

This distance, defined as the nonbonded radius sum, prescribes the structure packing. Within this framework, if the $M-O$ and $X-O$ distances increase, i.e., ionic radii from Shannon (40), the distortion of the tetrahedron chain will increase with the decrease of $M-O-X$ angle, θ, and the increase of the tilt angle, δ. This increase of constraints requires more energy to allow the $\alpha-\beta$ transition and its has thus been given a borderline value for the $\alpha-\beta$ transition: $\delta \sim 22°$ or $\theta \sim 136°$.

REFERENCES

1. A. Goiffon, J. C. Jumas, M. Maurin, and E. Philippot, *J. Solid State Chem.* **61**, 384 (1986).
2. J. C. Jumas, A. Goiffon, A. Zarka, B. Capelle, J. C. Doukhan, J. Schwartzel, J. Detaint, and E. Philippot, *J. Cryst. Growth* **80**, 133 (1987).
3. A. Goiffon, A. El Bouchikhi, J. C. Jumas, C. Avinens, M. Maurin, and E. Philippot, *Eur. J. Solid State Inorg. Chem.* **25**(2), 201 (1988).
4. E. Philippot, A. Goiffon, M. Maurin, J. Detaint, J. Schwartzel, Y. Toudic, B. Capelle, and A. Zarka, *J. Cryst. Growth* **104**, 713 (1990).
5. J. Detaint, H. Carru, J. Schwartzel, C. Joly, B. Capelle, A. Zarka, and E. Philippot, *Proc. Annu. Freq. Control Symp., 45th* **166** (1991).
6. J. Detaint, J. Schwartzel, C. Joly, B. Capelle, A. Zarka, Y. Zheng, Y. Toudic, and E. Philippot, *Proc. Eur. Freq. Time Forum, 6th* **223** (1992).
7. J. Detaint, J. Schwartzel, C. Joly, A. Zarka, B. Capelle, Y. Zheng, and E. Philippot, *Proc. Eur. Freq. Time Forum, 6th* **383**, (1992).
8. O. Cambon, A. Goiffon, and E. Philippot, *J. Mater. Sci.* **26**, 846 (1991).
9. O. Cambon, A. Goiffon, A. Ibanez, and E. Philippot, *J. Solid State Chem.* **103**, 240 (1993).
10. M. Deleuze, A. Goiffon, A. Ibanez, E. Philippot, *Proc. Eur. Freq. Time Forum, 7th* **255** (1993).
11. D. Cachau, J. Bennazha, A. Goiffon, A. Ibanez, and E. Philippot, *Eur. J. Solid State Inorg. Chem.* **29**, 1295 (1992).
12. E. Philippot, A. Ibanez, A. Goiffon, M. Cochez, A. Zarka, B. Capelle, J. Schwartzel, and J. Detaint, *J. Cryst. Growth* **130**, 195 (1993).
13. G. Dolino, J. P. Bacheimer, F. Gervais, and A. F. Wright, Bull. Mineral. **106**, 267 (1983).
14. T. Rey, Z. Kristallogr. **123**, 263 (1966).
15. E. C. Shafer, and R. Roy, *J. Am. Ceram. Soc.* **39**, 330 (1956).
16. E. C. Shafer, M. W. Shafer, and R. Roy, Z. Kristallogr. **108**, 263 (1956).
17. K. Kosten and H. Arnold, Z. Kristallogr. **152**, 119 (1980).
18. E. Snoeck, C. Roucau, and P. St. Gregoire, *J. Phys.* **47**, 2041 (1986).
19. A. Zarka, B. Capelle, E. Philippot, and J. C. Jumas, *J. Appl. Cryst.* **19**, 477 (1986).
20. W. R. Beck, *J. Am. Ceram. Soc.* **32**, 147 (1949).
21. E. C. Shafer and R. Roy, *Z. Phys. Chem.* **11**, 30 (1957),.
22. L. H. Cohen and W. Klement, *Philos. Mag.* **39**(4), 399 (1979).
23. A. Perloff, *J. Am. Ceram. Soc.* **39**, 83 (1956).
24. J. D. Jorgensen, *J. Appl. Phys.* **49**, 5473 (1978).
25. Dindune, Konstants, and Ozolin, *Latv. PSR Zinat. Akad. Vestis, Kim. Ser.* **4**, 499, (1971).
26. J. M. Stanley, *Am. Mineral.* **41**, 947, (1956).
27. H. Grimm and B. Dorner, *J. Phys. Chem. Solids* **36**, 407 (1975).
28. A. F. Wright and M. S. Lehmann, *J. Solid State Chem.* **36**, 371 (1981).
29. G. S. Smith, P. B. Isaacs, *Acta Crystallogr.* **17**, 842 (1964).
30. A. Goiffon, J. C. Jumas, and E. Philippot, *Rev. Chim. Miner.* **23**, 99 (1986).
31. F. D'Yvoire and M. Ronis, *C. R. Acad. Sci. Paris* **267**, 955 (1968).
32. H. N. Ng and C. Calvo, *Can. J. Phys.* **54**, 638 (1975).
33. O. Baumgartner, A. Preisinger, P. W. Krempl, and H. Mang, Z. Kristallogr. **168**, 83 (1984).
34. O. Baumgartner, M. Behmer, and A. Preisinger, Z. Kristallogr. **187**, 125 (1989).
35. W. L. Bragg, *Philos. Mag.* **40**, 169 (1920).
36. L. S. Bartell, *Tetrahedron* **17**, 177 (1962).
37. C. Glidewell, *Inorg. Chim. Acta* **12**, 219 (1975).
38. O'Keeffe and B. G. Hyde, *Trans. Am. Crystallogr. Assoc.* **15**, 65 (1979).
39. O'Keeffe and A. Navrotsky, "Structure and Bonding in Crystals." Academic Press, New York, 1981.
40. R. D. Shannon and C. T. Prewitt, *Acta Crystallogr., Sect. B* **25**, 925 (1969).
41. G. S. Smith, *Acta Crystallogr.* **16**, 542 (1963).
42. K. Kihara, *Eur. J. Mineral.* **2**, 63 (1990).
43. G. F. Engel and P. W. Krempl, *Ferroelectrics* **54**, 9 (1984).
44. R. A. Young, Defense Documentation Center, rep. AD 276 235, Washington 25, DC (1962).
45. G. Engel, H. Klapper, P. Kremple, and H. Mang, *J. Cryst. Growth* **94**, 597 (1989).